

Journal of Rehabilitation in Civil Engineering

Journal homepage: <https://civiljournal.semnan.ac.ir/>

A Damage Detection Approach for Cable-Stayed Bridges Using Displacement Responses and Mahalanobis Distance

Mahtab Mohseni Moghaddam ¹; Ehsan Dehghani ^{2,*}; Maryam Bitaraf ³

1. Ph.D. Candidate, Department of Civil Engineering, University of Qom, Qom, Iran

2. Associate Professor, Faculty of Civil Engineering, University of Qom, Qom, Iran

3. Assistant Professor, Faculty of Civil Engineering, University of Tehran, Tehran, Iran

* Corresponding author: dehghani@qom.ac.ir

ARTICLE INFO

Article history:

Received: 12 February 2024

Revised: 26 May 2024

Accepted: 01 August 2024

Keywords:

Cable-stayed bridges;

Damage detection;

Displacement response;

Mahalanobis distance;

Structural health monitoring.

ABSTRACT

Given the crucial role of cable-stayed bridges in infrastructure, continuous health monitoring throughout their lifespan is imperative. To achieve this purpose, a damage detection approach for cable-stayed bridges under loading was presented. This method aimed to assess the condition of cable-stayed bridges through phase space analysis of time domain responses. Displacement responses were utilized to minimize the need for extensive sensor deployment. Damage was identified by analyzing variations in the Mahalanobis distance index curve between intact and damaged models. This method was evaluated for effectiveness through a numerical case study. The case study involved damage design in the deck and cables of the Puqian cable-stayed bridge. The results demonstrated that this method can efficiently detect the damage location in the cable-stayed bridge and exhibited anti-noise capability in identifying the location of damage, especially for cables. Its accuracy at a noise level of 30 dB was 76.5%, 5.56%, and 75% for cable, deck, and combined cable and deck scenarios, respectively. This method can serve as a rapid and continuous monitoring tool for damage detection in cable-stayed bridges, with minimal traffic disruption and relying solely on deck displacement responses.

E-ISSN: 2345-4423

© 2025 The Authors. Journal of Rehabilitation in Civil Engineering published by Semnan University Press.

This is an open access article under the CC-BY 4.0 license. (<https://creativecommons.org/licenses/by/4.0/>)

How to cite this article:

Mohseni Moghaddam, M., Dehghani, E., & Bitaraf, M. (2025). A Damage Detection Approach for Cable-Stayed Bridges Using Displacement Responses and Mahalanobis Distance. *Journal of Rehabilitation in Civil Engineering*, 13(2), 47-63. <https://doi.org/10.22075/jrce.2024.33273.1995>

1. Introduction

In recent years, numerous cable-stayed bridges have been built around the world for the smooth flow of traffic. The demand for large-scale bridges is on the rise owing to extensive global infrastructure development. Cable-stayed bridges, distinguished by their extended span and flexibility, exhibit unique characteristics in both static and dynamic behavior when compared to other engineering structures[1]. They are typically constructed along vital transportation routes and require regular maintenance to uphold their operational functionality and safety standards. Cable-stayed bridges encounter adverse environmental conditions, including strong winds, extreme temperatures, and heavy vehicle loads, posing challenges to the effective management and maintenance of these structures. Conventional inspections are costly in terms of both time and labor and often prove inadequate for effective bridge maintenance. Consequently, there is a growing preference for the adoption of Structural Health Monitoring (SHM) systems in the maintenance of long-span cable-stayed bridges. SHM can offer timely insights into bridge behavior, providing early warnings for potential hazards and facilitating damage assessment in critical components, including expansion joints, stay cables, and suspenders[2–4]. Inspecting cables, regarded as vital components, is a crucial aspect of certifying the health of cable-stayed bridges. Typically, both the dead and the live loads are transmitted straight to the towers via these cables. Furthermore, environmental factors, corrosion, vibrations, and fatigue can contribute to the degradation of cables, resulting in a decrease in their carrying capacity. Consequently, maintaining the force of the cables within the acceptable range significantly affects the overall stress of the bridge.

With the advancement of SHM, it became possible to monitor the health of cable-stayed bridges under various conditions, including thermal loads, ambient loads, vehicular loads, vibrations, and seismic events. The characteristics investigated for SHM of bridges, which typically include bridge responses such as displacement, strain, acceleration, support reactions, and modal parameters, were categorized into two groups: time domain and frequency domain.

Amidst various monitored parameters, displacement responses, recognized as sensitive indicators of applied loads on a structure, were employed to assess bridge performance. These responses are typically monitored using Global Positioning System (GPS) sensors and vision-based methods. In many studies, the mid-span displacement of cable-stayed bridges has been examined under traffic load and environmental factors, such as temperature, for health assessment[5–7]. Lei et al. explored a method for estimating the displacement response of a bridge under several loads through a residual auto-encoder model. Monitoring data from a cable-stayed bridge were gathered to verify the approach, encompassing measurements of diverse loads and displacement responses. The introduced approach aimed to provide early warning for potential failures in the bridge[8]. Wangchuk et al. conducted a study on the estimation of stay cable tension using vision-based measurements under ambient conditions. Microvibrations of the stay cable were captured by a video camera, and spatial displacements of the cable were extracted from sequences of cable images. Modal parameters of the cable were identified from the cable displacement responses. The proposed technique accurately estimated the tension of the stay cable based on the identified natural frequencies[9]. As mentioned, the health monitoring of cables in cable-stayed bridges was also evaluated through the structural response behavior and support reactions. This technique involved analyzing shear forces near the supports by measuring strains along the deck [10].

Vibration-based methods have been utilized in numerous studies for structural diagnosis and damage detection through modal parameters of bridges, such as natural frequency and mode shapes. These parameters were employed to assess the bridge's performance over time[11]. The

combination of machine learning with feature extraction methods such as Wavelet transform, Hilbert-Huang Transform (HHT), and Teager-Huang Transform (THT) was applied to map damage characteristics for damage detection[12]. Vibration-based methods were extensively employed for estimating cable tension and assessing the integrity of cable structures[13]. Natural frequency, as a general structural index, exhibited insensitivity to local damage. Mode shape and the indicators derived from it can be affected by environmental noise[14,15]. Conventional techniques based on natural frequency are insensitive to early levels of damage[16]. In operational conditions, these characteristics impose limitations on the detection of local bridge damage using vibration-based methods.

Damage detection methods based on Time Domain Response (TDR) were stronger in identifying local damage. In these methods, damage was recognized directly from the time domain response without the need to convert outputs to modal parameters. Consequently, the TDR directly reflected local bridge damage levels, and these methods exhibited higher sensitivity to local damage[17,18]. The motion of vehicles constitutes a primary factor influencing the behavior of highway bridges. Consequently, rather than relying on modal parameters, the detection of damage in bridges can be accomplished by analyzing time domain responses induced by the moving load. Output-only methods, including the fractal dimension of bridge responses, were explored for detecting damage in bridges caused by moving vehicles[19]. Acceleration responses from several vehicles were also utilized for bridge damage detection[20].

Zhang et al. suggested a technique for identifying damage in a bridge subjected to a moving load, leveraging alterations in phase trajectories. This approach involved the initial conversion of time-domain responses into a phase domain, allowing subtle variations in parameters to manifest throughout the entire system. Subsequently, the index was established as the distance between the trajectories of the damaged and undamaged states, providing insight into the location of the damage[21]. Nie et al. suggested a damage index based on Changes in Phase Space Topology (CPST) of responses of a two-span slab for structural damage identification. Except for responses measured at the supports, the CPST values based on the phase space response at other measurement points increased with the level of damage. CPST was much more sensitive to structural damage than modal parameters, even when the measurement point was far from the damage[22,23]. Peng et al. proposed an approach to enhance the capability of structural damage detection using the phase space topology technique based on Singular Spectrum Analysis (SSA). The dynamic acceleration response was decomposed by SSA. The proposed method was sensitive and reliable for detecting structural damage[24].

In multivariate statistical analysis, the Mahalanobis distance served as an additional indicator, measuring the distance in standard deviation scale between an observation and a reference sample. Similar to the CPST, it has been introduced as a damage indicator in health monitoring studies[25]. Pamwani and Shelke introduced a novel technique for structural health monitoring and damage detection using shockwave loading on a shear building. The proposed study utilized the dissimilarity of phase space trajectories of structural responses to extract two damage-sensitive features, namely, CPST and Mahalanobis distance. CPST and Mahalanobis distance were found to be strong, sensitive features capable of quantifying damage initiation and evolution[26]. The considerable sensitivity of phase space analysis to damage has led to its widespread application in numerous studies focused on detecting structural damage[27–30].

As mentioned, vibration-based methods often lead to prolonged traffic jams or bridge closures. Furthermore, studies have shown that modal parameters were less sensitive to local damage, while time domain responses were stronger under moving loads. This study introduced an approach to

assess and detect damage in the deck and cables of cable-stayed bridges by examining deck displacement during moving load with minimal traffic disruption. The proposed method for monitoring the health of the cable-stayed bridge investigated changes in the reconstructed responses within the phase space. The reconstruction in the phase space amplifies the changes in structural responses. Research in the field of damage detection using phase space topology has often been conducted on structures like buildings and highway bridges. The effectiveness of phase space analysis on cable-stayed bridges was evaluated using the Mahalanobis distance. This method provided a rapid approach for initial damage detection using only one response of the cable-stayed bridges. The displacements of the bridges can be easily measured and extracted by non-contact and vision methods (such as videography and photography). The emphasis of this approach was on high sensitivity to structural changes, continuous monitoring of the bridge with minimal traffic disruption, and eliminating the necessity for deploying numerous and costly sensors along the entire length of the deck. Mahalanobis distance index was computed using the displacement responses of the Puqian cable-stayed bridge under loading. The identification of the damage location was accomplished by comparing the normalized Mahalanobis distance curves in the damaged and intact states. The viability of the method has been demonstrated for both cable damage and deck damage cases, as well as cases involving a combination of cable and deck damage, through a numerical case study. The Signal-to-Noise Ratios (SNR) of 30 and 25 dB were incorporated to assess the method's resistance to noise interference. A flowchart summarizing the relevant literature and illustrating the progression leading to this research is provided in Figure 1.

In the following, the study is organized as: Section 2 describes the topology of the phase space, along with the reconstruction of responses and the Mahalanobis distance. Section 3 is dedicated to defining the cable-stayed bridge and its characteristics. Section 4 provides details of the numerical simulation of the proposed method and presents the results. Finally, the conclusion is presented in Section 5.

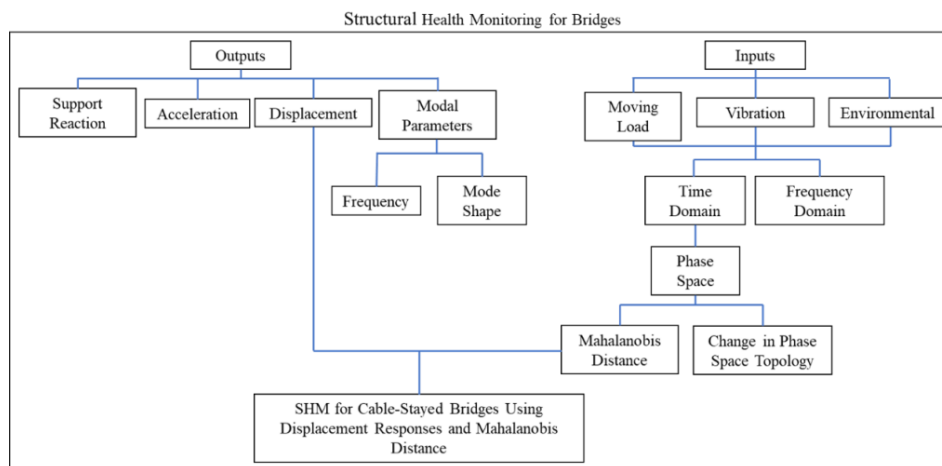


Fig. 1. Summary of relevant literature review.

2. Proposed approach for damage detection

Advanced sensor systems have facilitated the collection of extensive data for SHM and damage identification. Data mining plays a crucial role in the SHM of cable-stayed bridges, providing essential information to evaluate their structural condition and recognize potential damage[12]. In this study, the workflow of the proposed approach encompassed four steps: deck displacement extraction, reconstructing structural responses in phase space to magnify changes, investigating damage features, and ultimately detecting damage.

2.1. Reconstruction of the phase trajectory

In a phase space, any variable within the system can be depicted as an axis in a multidimensional space. A system with one dimension is referred to as a phase line, while a two-dimensional system is termed a phase plane, and a three-dimensional system is denoted as a three-dimensional phase space. The description of any dynamical system can be expressed within a phase space, which can be reconstructed based on the measured time domain responses[21].

Phase space reconstruction may involve multiple responses measured in the time domain, including displacement, velocity, or acceleration, or it may consist of a single response measured in the time domain. For this purpose, the time series of a measured response was concatenated 'd' times, each with a delay equal to 'T'. Therefore, at any given time n, the reconstruction of the phase space can be expressed as follows:

$$X(n) = [x(n), x(n + T), \dots, x(n + (d - 1)T)] \quad (1)$$

Here, d represents the embedding dimension, and T denotes the time delay. This reconstruction method is commonly referred to as the delay method[27]. Selecting an appropriate time delay in the reconstruction process is crucial. The time lag can be determined using methods such as the Autocorrelation Function and the Average Mutual Information Function (AMIF). Typically, the delay for reconstruction is selected as the time corresponding to the first zero crossing of the autocorrelation function or the first minimum of the AMIF[31,32]. Similarly, the proper selection of the embedding dimension (d) is important in the reconstruction process. The appropriate embedding dimension is determined using notable techniques such as Singular System Analysis (SSA) and False Nearest Neighbor (FNN) methods[33,34].

2.2. Damage detection with change in phase trajectory

Damage induces alterations in the local structural stiffness, leading to changes in the distance between corresponding points along the trajectories of the damaged and undamaged models when a moving load traverses the damaged location. The phase trajectory of the intact model serves as the baseline, and a damage index, determined by the shift in phase space trajectories, is utilized to detect damage in the structure. The CPST is an indicator widely employed for damage detection.

In this study, an alternative damage-sensitive index was explored, focusing on measuring the probability distance between phase portraits. This method was notably simpler to calculate compared to the conventional CPST. The probabilistic distance measure employed in this context was the Mahalanobis distance. Traditionally, Mahalanobis distance assesses the distance of a point from a distributed set of points to determine its deviation from a representative population. In this paper, the damage-sensitive index, Mahalanobis distance, as presented by George et al., was utilized to evaluate the distance between phase portraits [35].

The observation vector for each point in both the undamaged and damaged models can be represented as matrices [X] and [Y] following the reconstruction of the phase portraits of the structural responses. These matrices possess dimensions of (m × d), where the number of columns (d) represents the embedding dimensions, and the number of rows (m) represents the sampled points in the embedded phase portrait. Undamaged and damaged phase portraits are represented by two random vectors, {X} and {Y}, respectively. The center of these portraits is determined by calculating the average of the corresponding random vectors, denoted as $\{\mu\}_X$ and $\{\mu\}_Y$, respectively. Their covariance matrices, denoted as $[C_{XX}]$ and $[C_{YY}]$, can also be estimated. To calculate the Mahalanobis distance, a single weighted covariance matrix is obtained by assigning relative weights to each of these covariance matrices. It is expressed as follows:

$$[C_{WW}] = W_1[C_{XX}] + W_2[CYY] \quad (2)$$

The weight factors are determined based on the ratio of the number of sampled points in each phase portrait to the total number of points in both models. In this paper, equal weights were assigned to each parameter, $W_1=W_2=0.5$. Subsequently, the Mahalanobis distance between the phase portraits is calculated using the following formula:

$$MD = \sqrt{(\{\mu\}_X - \{\mu\}_Y)^T [C_{WW}] (\{\mu\}_X - \{\mu\}_Y)} \quad (3)$$

More comprehensive details on calculating Mahalanobis distance can be found in the literature[35].

3. The case study bridge

In this study, the Puqian cable-stayed bridge, situated in the northeast of Hainan Province, China, was investigated. This bridge is a symmetrical single-tower cable-stayed bridge with two 230-meter spans, as depicted in Figure 2[36]. The cable-stayed bridge features an A-shaped concrete tower with a total height of 150 meters and a width of 60 meters at the foundation level. The transverse square beam of the tower is situated at a height of 34 meters, and its two slanted legs intersect at a height of 106 meters. Hollow rectangular boxes are used for the lower and middle parts of the tower. The deck comprises a closed steel box with a width of 37.5 meters and a height of 3.2 meters in the middle span. It is supported by two concert side bents at the ends of the spans and the transverse beam of the tower. Sixty-eight parallel wire cables are employed in the fan model to provide support to the deck. The cross-section and the initial tension force of the cables are detailed in Table 1. The concert side bent forms a portal frame with dimensions of 34 meters in height and 25 meters in width. Spherical steel bearings connect the deck to the bents and the tower. These bearings enable the bridge to slide longitudinally while remaining fixed to the side piers and tower in the transverse direction[36–38]. Table 2 presents the properties of the materials used in the investigated bridge.

Table 1. Design parameters of cables.

Cable No.	A (mm^2)	F_0 (kN)	Cable No.	A (mm^2)	F_0 (kN)
1	81.2	4129.9	10	48.9	2459.4
2	81.2	3835.0	11	48.9	2331.3
3	72	3631.9	12	48.9	2199.1
4	72	3423.9	13	42	2079.4
5	72	3240.4	14	42	1947.1
6	58.1	3112.9	15	35	1836.8
7	58.1	2934.5	16	35	1724.2
8	58.1	2768.5	17	42	2034.3
9	58.1	2602.6		48.9	

Table 2. Material properties of Puqian bridge[37].

Structural Components	Material	Elastic modulus (GPa)	Yield stress (MPa)	Density (kg/m^3)
Tower and bents	Concrete	34.5	32.5	2600
	Steel bar	210	400	7850
Deck	Steel plate	210	345	7850
Cables	Steel strand	195	1860	7850

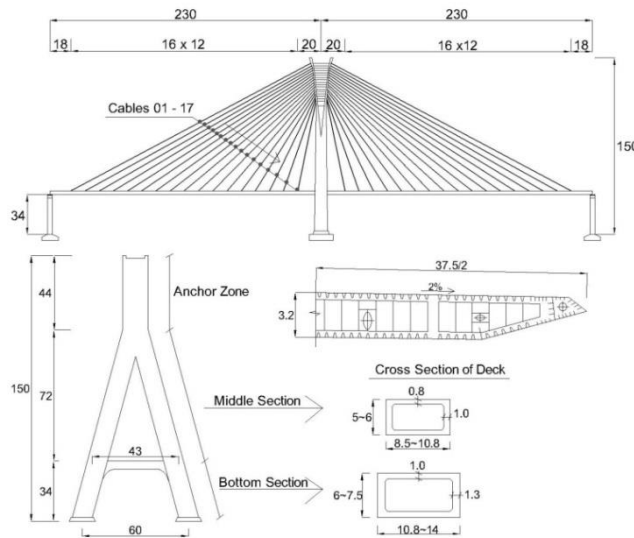


Fig. 2. Schematic of Puqian cable-stayed bridge. (unit: m).

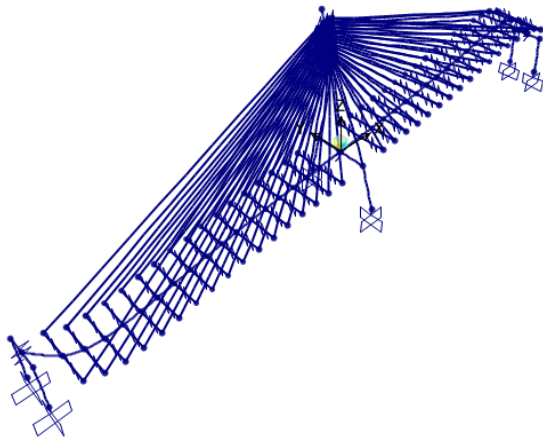
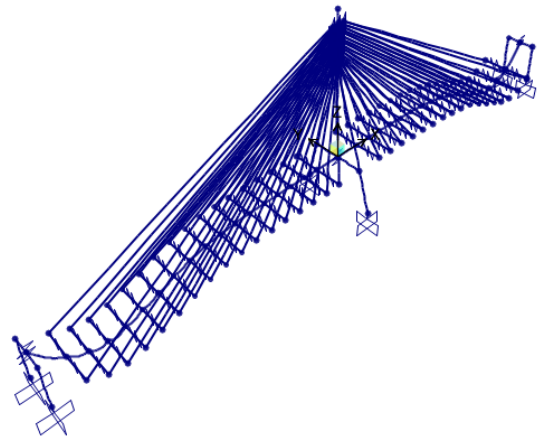
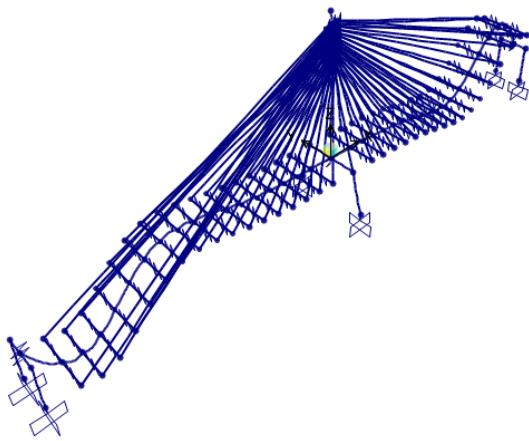
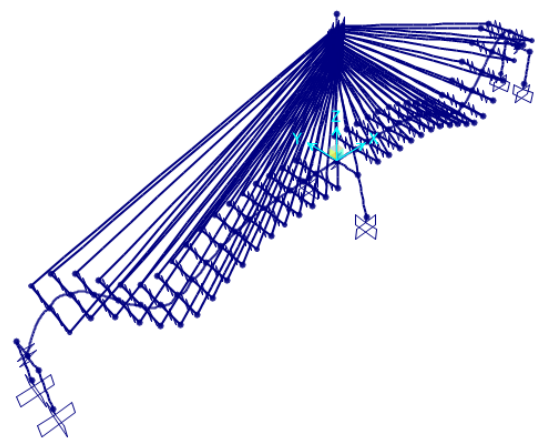
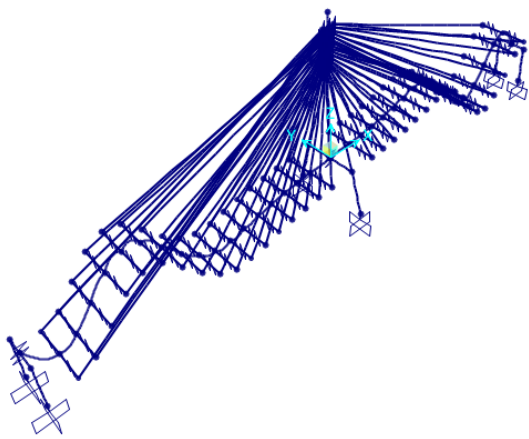
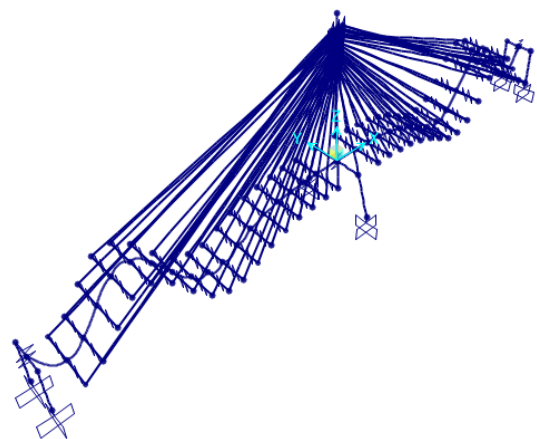
4. Numerical simulation

A numerical simulation was conducted using SAP2000 software for the initial evaluation of the method. The deck and pylon sections were modeled with frame elements, and cables were represented with cable elements. The finite element modeling made the following assumptions: (1) the deck was continuous, (2) the cables bore only axial forces, and (3) the analysis was conducted as a static time history with the neglect of dynamic effects. The calculated six natural frequencies and mode shapes are shown in Figure 3. Assuming that the deck was partitioned into 36 sections, as illustrated in Figure 4, each section was equipped with a displacement sensor positioned at the center of the section. Each sensor measured the displacement responses resulting from changes in one section of the deck and the two adjacent cables. The location of sensors along the bridge deck, with their respective deck sections and cables, are provided in Table 3.

A five-axle load similar to the Type 3-S2 of AASHTO legal loads was employed in the finite element model to simulate the interaction of the bridge with a vehicle[39]. This five-axle truck is also presented in the Australian Bridge Design Code as T44[40]. As illustrated in Figure 5, the moving load was applied to the deck through the distribution of multiple point loads at uniform intervals, and their corresponding time history function. Point loads were applied and removed from the deck. The loads successively passed over the bridge with a time difference Δt resulting from the distance between point loads and the speed of the moving load.

Table 3. Location of sensors, covered deck sections, and associated cables.

Deck No.	Cable No.	Sensor Location(m)	Deck No.	Cable No.	Sensor Location(m)	Deck No.	Cable No.	Sensor Location(m)
1	1	9	13	12 & 13	156	25	23 & 24	316
2	1 & 2	24	14	13 & 14	168	26	24 & 25	328
3	2 & 3	36	15	14 & 15	180	27	25 & 26	340
4	3 & 4	48	16	15 & 16	192	28	26 & 27	352
5	4 & 5	60	17	16 & 17	204	29	27 & 28	364
6	5 & 6	72	18	17 & PLYN	220	30	28 & 29	376
7	6 & 7	84	19	PLYN & 18	240	31	29 & 30	388
8	7 & 8	96	20	18 & 19	256	32	30 & 31	400
9	8 & 9	108	21	19 & 20	268	33	31 & 32	412
10	9 & 10	120	22	20 & 21	280	34	32 & 33	424
11	10 & 11	132	23	21 & 22	292	35	33 & 34	436
12	11 & 12	144	24	22 & 23	304	36	34	451

Mode 1, $FREQ = 0.30015$ Mode 2, $FREQ = 0.66142$ Mode 3, $FREQ = 0.73947$ Mode 4, $FREQ = 0.77442$ Mode 5, $FREQ = 0.84197$ Mode 6, $FREQ = 0.88062$ **Fig. 3.** 3D Finite element model and modes of the Puqian cable-stayed bridge.

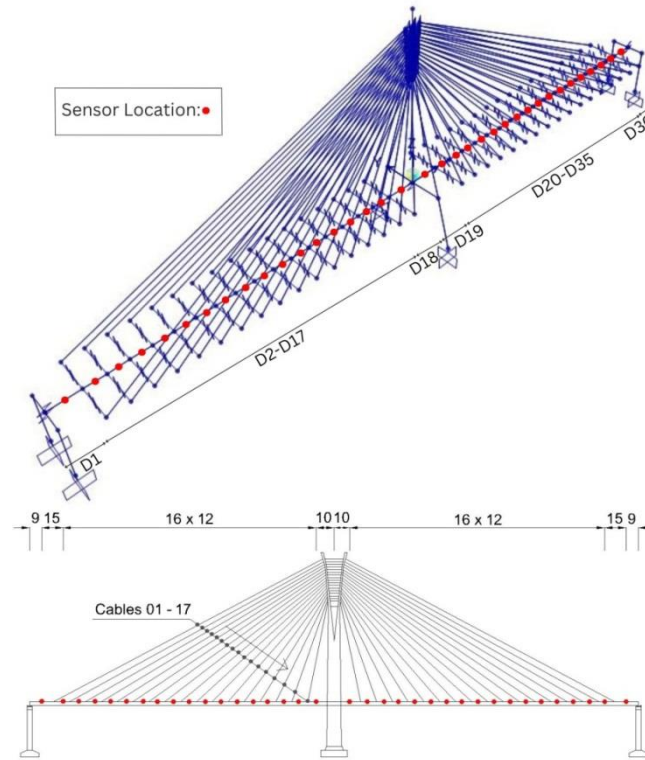


Fig. 4. Sensors arrangement. (unit: m).

For cables, damage can be caused by corrosion, fatigue, vehicle impact, or other factors. In each case, stiffness decreases, and the force of the cable changes. In this study, damage extent was defined as the percentage reduction in the stiffness of the cable-stayed bridge. The cases of damage to the cable were equalized by either removing or reducing the cross-section of the cables. Damage to the deck was also considered by reducing the moment of inertia of the deck. For all cable and deck sections, various damage extents from 10% to 40% had been analyzed. For example, 39 damage scenarios were chosen as per the specifications outlined in Table 4.

Table 4. Designed Damage cases.

Case No.	Cable or Deck No.	Damage Extent (%)	Case No.	Cable or DeckNo.	Damage Extent (%)
1	C1	30%	21	D8	40%
2	C3	20%	22	D10	30%
3	C5	10%	23	D12	20%
4	C7	40%	24	D14	20%
5	C9	20%	25	D16	10%
6	C11	20%	26	D18	40%
7	C13	30%	27	D20	40%
8	C15	10%	28	D22	10%
9	C17	20%	29	D24	20%
10	C19	30%	30	D26	30%
11	C21	40%	31	D28	20%
12	C23	40%	32	D30	10%
13	C25	10%	33	D32	40%
14	C27	30%	34	D34	10%
15	C29	20%	35	D36	40%
16	C31	10%	36	C1 – D28	25%
17	C33	40%	37	C7 – D20	25%
18	D2	20%	38	C21 – D17	25%
19	D4	20%	39	C30 – D1	25%
20	D6	10%			

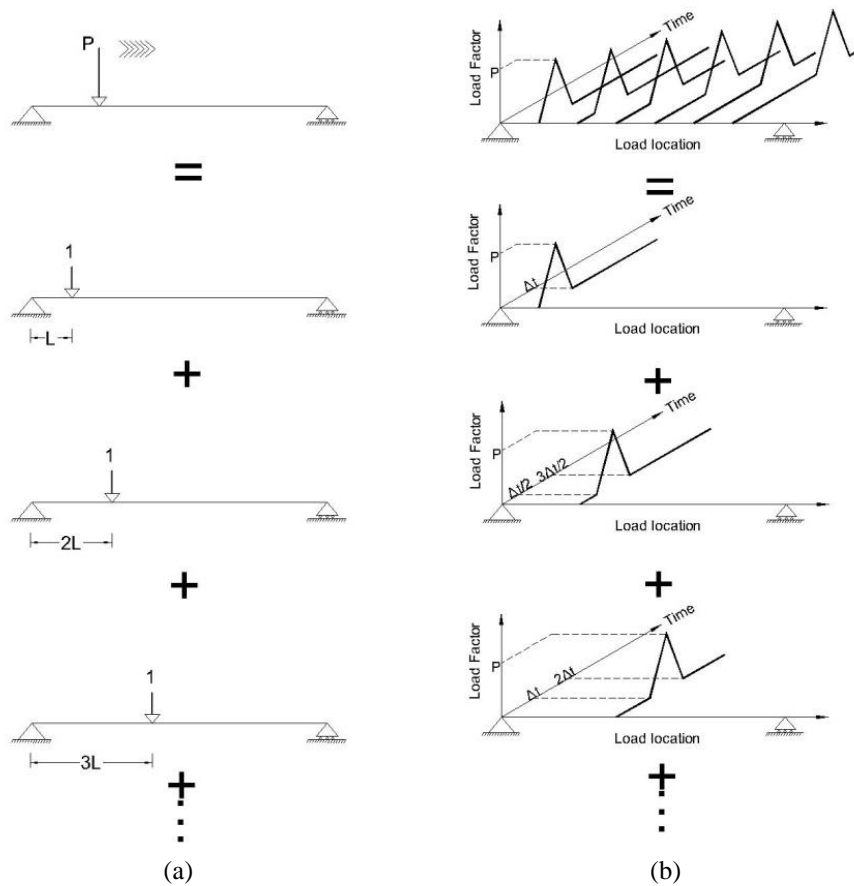


Fig. 5. (a) Point loads at uniform intervals and (b) The time history functions.

Cases 1-17 involved single cable damage, with damage rates ranging from 10% to 40%. Cases 18-35 represented single damage scenarios for the bridge deck, with damage levels varying between 10% and 40%. Cases such as 1, 9, 17, 26, and 35 were investigated to evaluate the efficiency of the method in detecting damage in the sections near the support and pylon. In cases 36-39, there was a combination of cable and deck damage, and these sections were not adjacent. The two damaged sections of the cable and the deck were positioned on both sides of the pylon. The combined damage cases included a backstay cable (1), and a near-pylon cable (21). The truck was applied to the model in both the undamaged state and each of the 39 damage scenarios separately. The sampling frequency and damping ratio of 0.1s and 5%, respectively, were used for the time history analysis. Displacement responses were recorded for each of the 36 sections. The displacement of each section was reconstructed in the phase space using the time delay and embedding dimensions obtained from the time series of the measured displacement. The reconstructed displacement of each point was $[X]$ and $[Y]$ for the undamaged and damaged models, respectively. The Mahalanobis distance between the phase portraits of the undamaged and damaged models was obtained using Eq. (3). Gaussian noise was added to the displacement responses to simulate measurement errors. The noise was considered using MATLAB software at two noise levels, SNR = 25 dB and SNR = 30 dB.

4.1. Results and discussion

Mahalanobis distance curves were computed using the equations outlined in section 2.2. Figure 6 illustrates the normalized Mahalanobis distance curves calculated for 17 cable damage cases without noise and with noise levels of 25 dB and 30 dB.

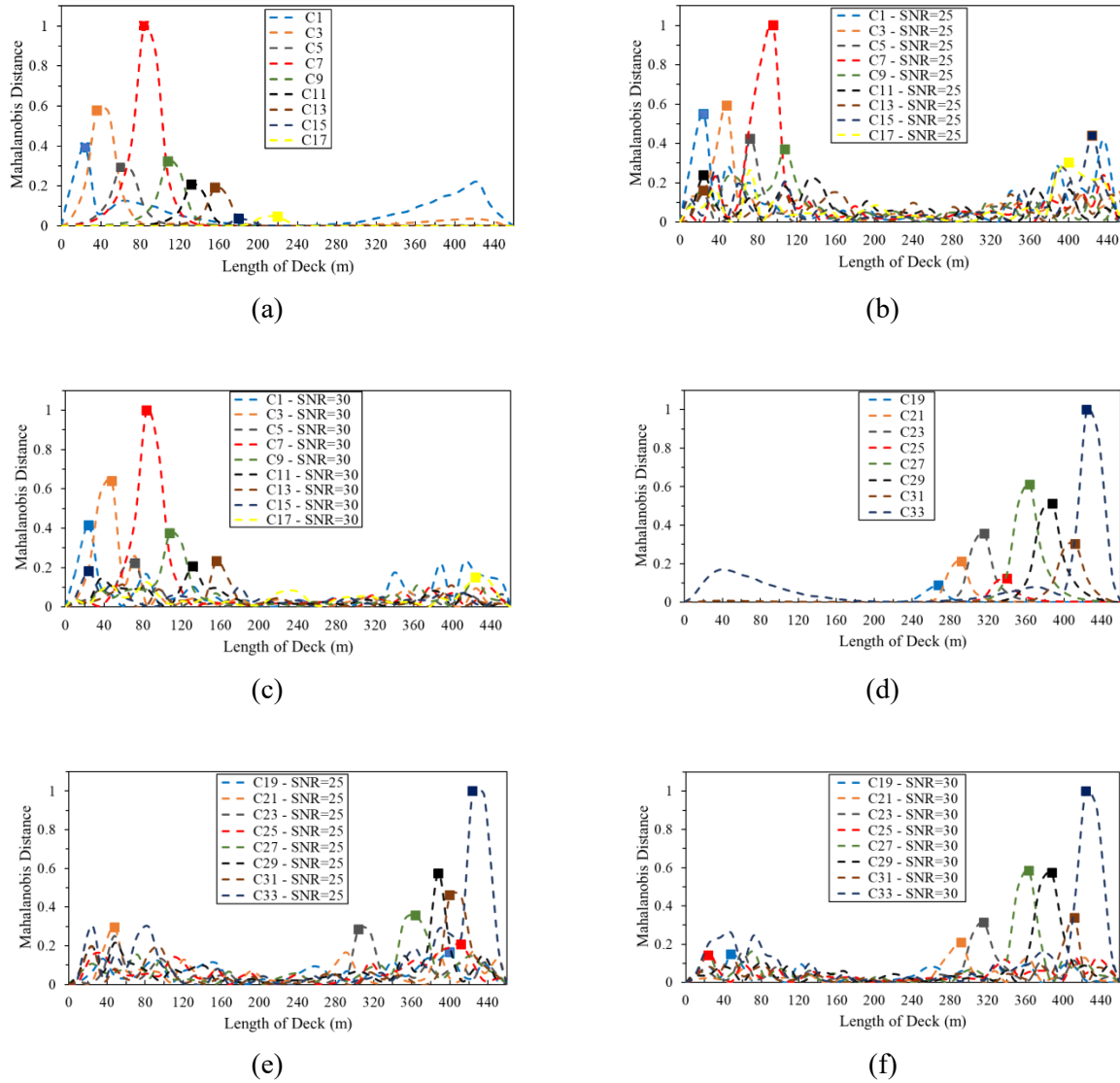


Fig. 6. Normalized Mahalanobis distance curves: (a) cases 1-9, (b) cases 1-9 (SNR = 25), (c) cases 1-9 (SNR = 30), (d) cases 10-17, (e) cases 10-17 (SNR = 25), (f) cases 10-17 (SNR = 30).

Upon applying damage to the bridge model, the displacement responses changed, and due to the dissimilarity of the phase portraits, the Mahalanobis distance curve experienced an increase from zero. As depicted in Figures 6(a) and (d), the Mahalanobis distance dramatically rose at specific points, and the location of the damaged cable was indicated by a conspicuous bulge. This bulge was well aligned with the location of the cables in the damaged cases. Moreover, the degree of bulging in the curves varied among different cases, with the maximum observed in the curves associated with cables 7 and 33. Comparing the values of Mahalanobis distance for different extents of damage showed that the degree of protrusion increases with the increase in damage extent. The curves related to cables 21 and 23, which had a 40% extent of damage similar to cables 7 and 33, exhibited a lower degree of bulging. These cables are closer to the pylon compared to cables 7 and 33. The degree of curve bulging of the cables that experienced the same damage intensity was different depending on the location of the cable. For example, at a damage extent of 10%, the normalized Mahalanobis distance values for cables 5, 15, 25, and 31 were 0.29, 0.035, 0.12, and 0.3, respectively. As shown in Figure 6(a), the lowest value was observed for cable 15, which is located near the left side of the pylon.

The Mahalanobis distance curve rose less near the support and the pylon compared to the increase observed in the portion farther from the pylon. The cables near the support, such as backstay cables, exhibited more complex behavior than the other cables. Like the support for all cables, they were affected by any changes made to the bridge and other cables. Additionally, due to the higher bending stiffness of the deck compared to that of the cables near the pylon, minimal displacement changes were observed for the cables near the pylon. The reduction in the degree of bulging in cables near the pylon was greater than that observed in backstay cables. This difference was evident in the comparison of cables 15 and 31 at a damage extent of 10%, cables 3 and 17 at 20% damage extent, cables 1 and 19 at 30% damage extent, and cables 21 and 33 at 40% damage extent.

The method's ability to tolerate noise was also investigated by adding 25 dB and 30 dB SNR to the displacement responses. Mahalanobis distance curves for 17 cable damage cases under 25 dB and 30 dB SNR are presented in Figure 6(b), (c), (e), and (f), respectively. In some cases, Mahalanobis distance values did not align perfectly, exhibiting fluctuations attributable to the addition of noise. This difference was more noticeable at 25 dB SNR. The bulging of the Mahalanobis distance curve for cable damage cases 11, 13, 15, 17, 19, 21, and 25 at the 25 dB SNR, as well as cable damage cases 15, 17, 19, and 25 at the 30 dB SNR, did not correspond with the location of the damaged cable. Cables 15, 17, 19, 21, and 25 exhibited the least level of protrusion in the noiseless state. The damage extent of these cables varied between 10% and 40%. Cable 21, which had the highest damage extent compared to the others, was also detected at a noise level of 30 dB. Significant peaks were observed in the curves of other cable damage cases, including backstay cables, particularly at the 30 dB noise level, and the location of the damaged cable was accurately identified. The Mahalanobis distance identification accuracy for scenarios of damaged cables in the noise levels of 30 and 25 dB was 76.5%, and 58.8%, respectively. The normalized Mahalanobis distance curves calculated for 18 bridge deck damage cases, both without noise and with noise levels of 25 dB and 30 dB, are presented in Figure 7.

The variations in the curve for damage cases designed for decks were more noticeable compared to those associated with cables. This issue was particularly heightened in sections close to the supports. However, as depicted in Figure 7(a) and (d), the Mahalanobis distance curves exhibited more prominent bulges at specific points. Except for the damage case related to deck 36, all bulges aligned precisely with the location of the damaged section of the bridge deck. Deck 36 is the section connected to the right support of the bridge. A rise in Mahalanobis distance values was directly linked to an increase in the extent of damage. However, similar to the cables near the pylon, the curve changes for the sections near the pylon showed a distinct behavior compared to other sections of the deck. For instance, the values of bulging for deck sections 18 and 20, designed with 40% damage, were 0.089 and 0.02, respectively. The Mahalanobis distance value for deck section 8, with the same 40% damage extent, reached the maximum value of 1. Deck sections 6, 30, and 34 were also well identified at a low damage extent of 10%, with damage index values of 0.28, 0.15, and 0.18, respectively.

The efficiency of the proposed approach is illustrated in Figures 7(b), (c), (e), and (f) under the influence of 25 dB and 30 dB noise for 18 deck damage cases. Significant fluctuations were observed in the Mahalanobis distance curve for the damage cases designed for the deck under noise. As a result, none of the curved bulges aligned with the location of the damaged deck at the noise level of 25 dB. It was inferred that the displacement response of the bridge to damage in the deck sections was more susceptible to the influence of noise. The accuracy of Mahalanobis distance in identifying scenarios of the damaged deck at the noise level of 30 dB was 5.56%. Figure 8(a)

depicts the normalized Mahalanobis distance curve for the combination cases involving damage to cable and deck sections.

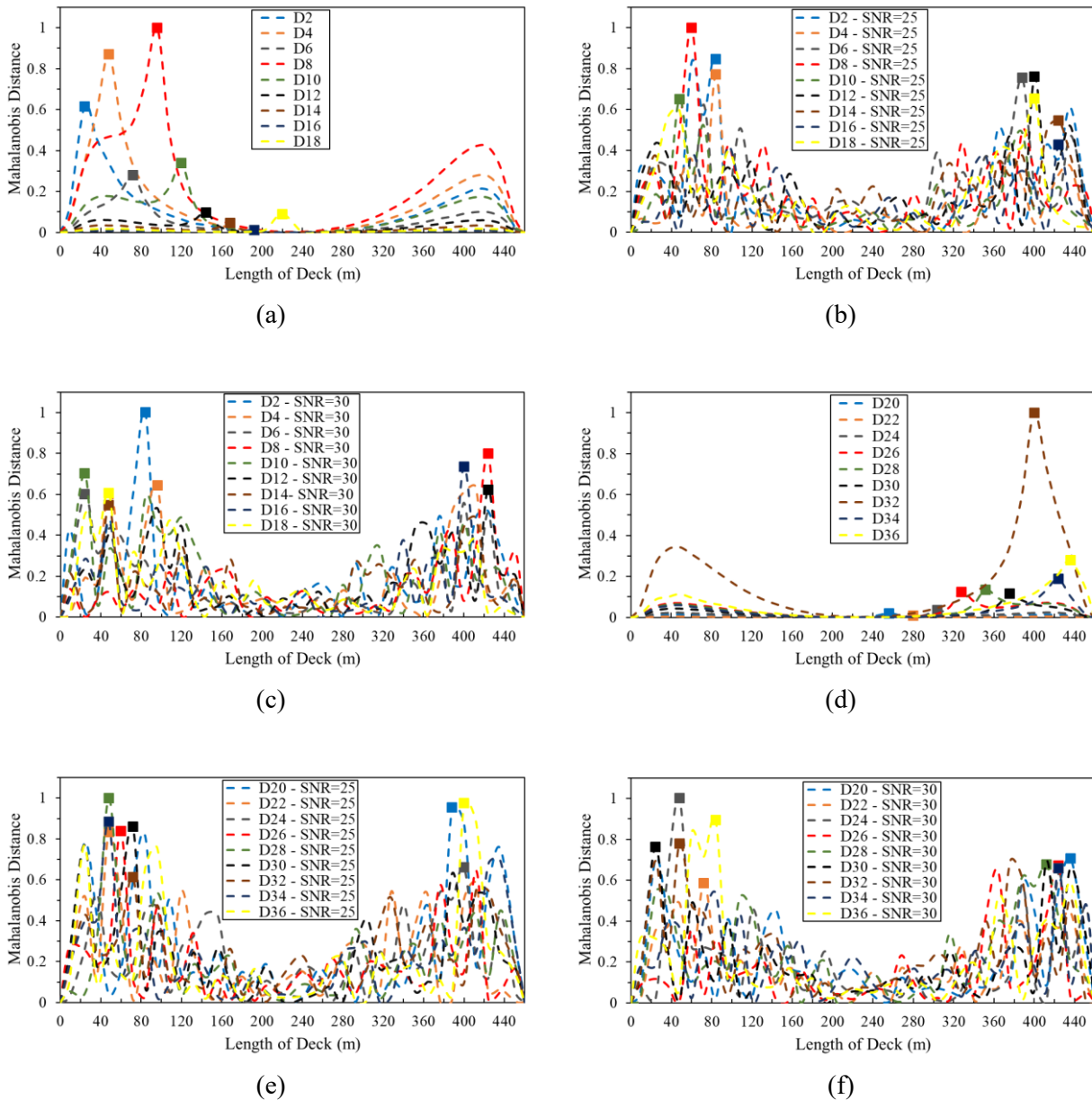


Fig. 7. Normalized Mahalanobis distance curves: (a) cases 18-26, (b) cases 18-26 (SNR = 25), (c) cases 18-26 (SNR = 30), (d) cases 27-35, (e) cases 27-35 (SNR = 25), (f) cases 27-35 (SNR = 30).

The curve indicated that for cases with combined damage, the damage index easily identified the location of the damaged cable, similar to the cable damage cases. However, the damaged section of the deck was not detected. Another noteworthy observation was the varying degree of bulging observed for the same amount of damage across all four combined damage cases. The Mahalanobis distance values varied depending on the distance of the damaged cable from the support and the pylon, regardless of the location of the damaged deck section. The highest value of the Mahalanobis distance related to the damage case involving the cable was 30. The damaged cases involving cable 21 and deck 17 exhibited the least change in the Mahalanobis distance value, possibly attributed to the proximity of cable 21 to the pylon compared to the other considered cables. Afterward, the case involving the backstay cable exhibited the lowest degree of protrusion.

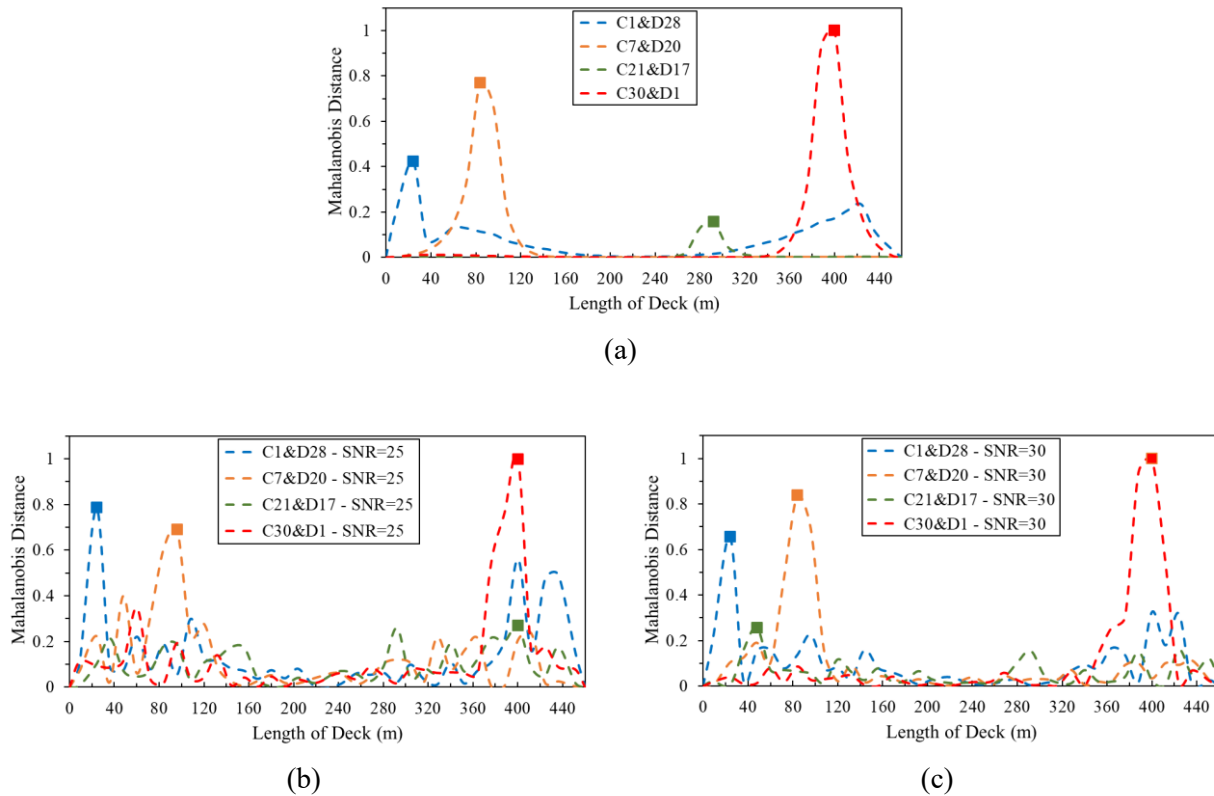


Fig. 8. Normalized Mahalanobis distance curves: (a) cases 36-39, (b) cases 36-39 (SNR = 25), (c) cases 36-39 (SNR = 30).

As depicted in Figure 8(b) and (c), in the presence of noise, cases of combined damage exhibited fewer fluctuations. Additionally, most of the curve bulges aligned well with the damaged cable area. In the curves of three damage cases, C7&D20 and C21&D17 at 25 dB SNR, and C21&D17 at 30 dB SNR, the location of the damaged cable did not align with the bulging location. The Mahalanobis distance was able to identify only the damaged cable, both in the absence and presence of noise. At noise levels of 30 and 25 dB, 75% and 50% of the combined damaged scenarios were detected, respectively.

5. Conclusion

In this paper, a method for detecting damage in a cable-stayed bridge under loading using the deck displacement response in the time domain and phase space theory was presented. A numerical simulation of the Puqian cable-stayed bridge was conducted to validate the proposed method under 39 damage cases including cable and deck damage. The results are summarized as follows:

- Mahalanobis distance accurately identified all cable and deck scenarios at damage levels ranging from 10% to 40%. In cases involving a combination of deck and cable damage, it was feasible only to determine the location of the damaged cable. Damage to cable exhibited a more significant effect on the Mahalanobis distance index compared to deck damage.
- The value of Mahalanobis distance in both damage scenarios for cables and deck sections near the pylon and supports was lower than that at other points, even at a damage intensity of 40%.
- This damage index exhibited anti-noise capability. Its accuracy at the noise level of 30 dB was 76.5%, 5.56%, and 75% for cable, deck, and combined cable and deck scenarios, respectively. At the noise level of 25 dB, 58.8% and 50% of the damaged cable scenarios and combinations

of cable and deck scenarios were detected, respectively. The detection accuracy diminished at 25 dB SNR. In cases involving damage to deck sections, the accuracy of the Mahalanobis distance index at 25 dB SNR was nearly zero.

This paper introduced the basic concept of rapid damage detection in cable-stayed bridges using the proposed method, but it also had some limitations. The feasibility of this method should be validated through additional experiments in the future. Several parameters, such as the load pattern (including axle configurations, speed, weight, etc.), the location of the sensor and the truck in the transverse lines of the deck, and the consideration of environmental factors like temperature, can be explored in future studies. These investigations have the potential to enhance the accuracy of the proposed method.

Funding

This research did not receive any specific external grant.

Conflicts of interest

The authors declare that they have no known competing financial interests or personal relationships that could have appeared to influence the work reported in this paper.

Authors contribution statement

Mahtab Mohseni Moghaddam: Writing - original draft, Writing - review & editing, Software, Formal analysis, Data curation, Investigation.

Ehsan Dehghani: Review & editing, Conceptualization, Resources, Methodology, Validation, Supervision, Project administration.

Maryam Bitaraf: Review & editing, Conceptualization, Methodology, Validation, Supervision, Project administration.

References

- [1] Zhang L, Qiu G, Chen Z. Structural health monitoring methods of cables in cable-stayed bridge: A review. *Measurement* 2021;168:108343. <https://doi.org/10.1016/j.measurement.2020.108343>.
- [2] Zhang Y-M, Wang H, Bai Y, Mao J-X, Chang X-Y, Wang L-B. Switching Bayesian dynamic linear model for condition assessment of bridge expansion joints using structural health monitoring data. *Mechanical Systems and Signal Processing* 2021;160:107879. <https://doi.org/10.1016/j.ymsp.2021.107879>.
- [3] Li S, Niu J, Li Z. Novelty detection of cable-stayed bridges based on cable force correlation exploration using spatiotemporal graph convolutional networks. *Structural Health Monitoring* 2021;20:2216–28. <https://doi.org/10.1177/1475921720988666>.
- [4] Wang F, Ning S, Sun Z. Experimental investigation on wear resistance of bushing in bridge suspenders. *Journal of Performance of Constructed Facilities* 2020;34:06020001. [https://doi.org/10.1061/\(ASCE\)CF.1943-5509.0001429](https://doi.org/10.1061/(ASCE)CF.1943-5509.0001429).
- [5] Zhou Y, Sun L. Insights into temperature effects on structural deformation of a cable-stayed bridge based on structural health monitoring. *Structural Health Monitoring* 2019;18:778–91. <https://doi.org/10.1177/1475921718773954>.
- [6] Lei X, Siringoringo DM, Dong Y, Sun Z. Interpretable machine learning methods for clarification of load-displacement effects on cable-stayed bridge. *Measurement* 2023;220:113390. <https://doi.org/10.1016/j.measurement.2023.113390>.

- [7] Jesus A, Brommer P, Westgate R, Koo K, Brownjohn J, Laory I. Bayesian structural identification of a long suspension bridge considering temperature and traffic load effects. *Structural Health Monitoring* 2019;18:1310–23. <https://doi.org/10.1177/1475921718794299>.
- [8] Lei X, Siringoringo DM, Sun Z, Fujino Y. Displacement response estimation of a cable-stayed bridge subjected to various loading conditions with one-dimensional residual convolutional autoencoder method. *Structural Health Monitoring* 2023;22:1790–806. <https://doi.org/10.1177/14759217221116637>.
- [9] Wangchuk S, Siringoringo DM, Fujino Y. Modal analysis and tension estimation of stay cables using noncontact vision-based motion magnification method. *Structural Control and Health Monitoring* 2022;29:e2957. <https://doi.org/10.1002/stc.2957>.
- [10] Nazarian E, Ansari F, Azari H. Recursive optimization method for monitoring of tension loss in cables of cable-stayed bridges. *Journal of Intelligent Material Systems and Structures* 2016;27:2091–101. <https://doi.org/10.1177/1045389X15620043>.
- [11] Saidin SS, Kudus SA, Jamadin A, Anuar MA, Amin NM, Ya ABZ, et al. Vibration-based approach for structural health monitoring of ultra-high-performance concrete bridge. *Case Studies in Construction Materials* 2023;18:e01752. <https://doi.org/https://doi.org/10.1016/j.cscm.2022.e01752>.
- [12] Pan H, Azimi M, Yan F, Lin Z. Time-Frequency-Based Data-Driven Structural Diagnosis and Damage Detection for Cable-Stayed Bridges. *Journal of Bridge Engineering* 2018;23:04018033. [https://doi.org/10.1061/\(asce\)be.1943-5592.0001199](https://doi.org/10.1061/(asce)be.1943-5592.0001199).
- [13] Zarbaf SEHAM, Norouzi M, Allemang RJ, Hunt VJ, Helmicki A, Venkatesh C. Ironton-Russell Bridge: Application of Vibration-Based Cable Tension Estimation. *Journal of Structural Engineering* 2018;144:04018066. [https://doi.org/10.1061/\(asce\)st.1943-541x.0002054](https://doi.org/10.1061/(asce)st.1943-541x.0002054).
- [14] Wu B, Wu G, Lu H, Feng DC. Stiffness monitoring and damage assessment of bridges under moving vehicular loads using spatially-distributed optical fiber sensors. *Smart Materials and Structures* 2017;26:1–21. <https://doi.org/10.1088/1361-665X/aa5c6f>.
- [15] Hong W, Wu Z, Yang C, Wan C, Wu G. Investigation on the damage identification of bridges using distributed long-gauge dynamic macrostrain response under ambient excitation. *Journal of Intelligent Material Systems and Structures* 2012;23:85–103. <https://doi.org/10.1177/1045389X11430743>.
- [16] Le HT, Thammarak P. Damage detection of a reinforced concrete beam using the modal strain approach. *International Journal of Dynamics and Control* 2023;11:2774–85. <https://doi.org/10.1007/s40435-023-01160-2>.
- [17] Wu B, Wu G, Yang C. Parametric study of a rapid bridge assessment method using distributed macro-strain influence envelope line. *Mechanical Systems and Signal Processing* 2019;120:642–63. <https://doi.org/10.1016/j.ymssp.2018.10.039>.
- [18] He WY, Ren WX, Zhu S. Baseline-free damage localization method for statically determinate beam structures using dual-type response induced by quasi-static moving load. *Journal of Sound and Vibration* 2017;400:58–70. <https://doi.org/10.1016/j.jsv.2017.03.049>.
- [19] Zhang L, Wu G, Cheng X. A rapid output-only damage detection method for highway bridges under a moving vehicle using long-gauge strain sensing and the fractal dimension. *Measurement: Journal of the International Measurement Confederation* 2020;158:107711. <https://doi.org/10.1016/j.measurement.2020.107711>.
- [20] Sarwar MZ, Cantero D. Deep autoencoder architecture for bridge damage assessment using responses from several vehicles. *Engineering Structures* 2021;246:113064. <https://doi.org/10.1016/j.engstruct.2021.113064>.
- [21] Zhang W, Li J, Hao H, Ma H. Damage detection in bridge structures under moving loads with phase trajectory change of multi-type vibration measurements. *Mechanical Systems and Signal Processing* 2017;87:410–25. <https://doi.org/10.1016/j.ymssp.2016.10.035>.
- [22] Nie Z, Hao H, Ma H. Structural damage detection based on the reconstructed phase space for reinforced concrete slab: Experimental study. *Journal of Sound and Vibration* 2013;332:1061–78. <https://doi.org/https://doi.org/10.1016/j.jsv.2012.08.024>.

- [23] Nie Z, Hao H, Ma H. Using vibration phase space topology changes for structural damage detection. *Structural Health Monitoring* 2012;11:538–57. <https://doi.org/10.1177/1475921712447590>.
- [24] Peng Z, Li J, Hao H, Nie Z. Improving identifiability of structural damage using higher order responses and phase space technique. *Structural Control and Health Monitoring* 2021;28:e2808. <https://doi.org/10.1002/stc.2808>.
- [25] De Maesschalck R, Jouan-Rimbaud D, Massart DL. The mahalanobis distance. *Chemometrics and Intelligent Laboratory Systems* 2000;50:1–18. [https://doi.org/10.1016/S0169-7439\(99\)00047-7](https://doi.org/10.1016/S0169-7439(99)00047-7).
- [26] Pamwani L, Shelke A. Damage Detection Using Dissimilarity in Phase Space Topology of Dynamic Response of Structure Subjected to Shock Wave Loading. *Journal of Nondestructive Evaluation, Diagnostics and Prognostics of Engineering Systems* 2018;1:1–13. <https://doi.org/10.1115/1.4040472>.
- [27] Tuttipongsawat P, Sasaki E, Suzuki K, Fukuda M, Kawada N, Hamaoka K. PC tendon damage detection based on phase space topology changes in different frequency ranges. *Journal of Advanced Concrete Technology* 2019;17:474–88. <https://doi.org/10.3151/jact.17.474>.
- [28] Paul B, George RC, Mishra SK. Phase space interrogation of the empirical response modes for seismically excited structures. *Mechanical Systems and Signal Processing* 2017;91:250–65. <https://doi.org/10.1016/j.ymsp.2016.12.008>.
- [29] Peng Z, Li J, Hao H. Data driven structural damage assessment using phase space embedding and Koopman operator under stochastic excitations. *Engineering Structures* 2022;255:113906. <https://doi.org/10.1016/j.engstruct.2022.113906>.
- [30] Peng Z, Li J, Hao H. Structural damage detection via phase space based manifold learning under changing environmental and operational conditions. *Engineering Structures* 2022;263:114420. <https://doi.org/10.1016/j.engstruct.2022.114420>.
- [31] Abarbanel H. *Analysis of observed chaotic data*. New York (NY): Springer; 2012.
- [32] Jiang A-H, Huang X-C, Zhang Z-H, Li J, Zhang Z-Y, Hua H-X. Mutual information algorithms. *Mechanical Systems and Signal Processing* 2010;24:2947–60. <https://doi.org/10.1016/j.ymsp.2010.05.015>.
- [33] Broomhead DS, King GP. Extracting qualitative dynamics from experimental data. *Physica D: Nonlinear Phenomena* 1986;20:217–36. [https://doi.org/10.1016/0167-2789\(86\)90031-X](https://doi.org/10.1016/0167-2789(86)90031-X).
- [34] Rhodes C, Morari M. The false nearest neighbors algorithm: An overview. *Computers & Chemical Engineering* 1997;21:S1149–54. [https://doi.org/10.1016/S0098-1354\(97\)87657-0](https://doi.org/10.1016/S0098-1354(97)87657-0).
- [35] George RC, Mishra SK, Dwivedi M. Mahalanobis distance among the phase portraits as damage feature. *Structural Health Monitoring* 2018;17:869–87. <https://doi.org/10.1177/1475921717722743>.
- [36] Yi J, Yu D. Longitudinal damage of cable-stayed bridges subjected to near-fault ground motion pulses. *Advances in Bridge Engineering* 2021;2:1–22. <https://doi.org/10.1186/s43251-021-00034-x>.
- [37] Yi J, Li J. Longitudinal Seismic Behavior of a Single-Tower Cable-Stayed Bridge Subjected to Near-Field Earthquakes. *Shock and Vibration* 2017;2017. <https://doi.org/10.1155/2017/1675982>.
- [38] Zhu L, Zhou Q, Ding Q, Xu Z. Identification and application of six-component aerodynamic admittance functions of a closed-box bridge deck. *Journal of Wind Engineering and Industrial Aerodynamics* 2018;172:268–79. <https://doi.org/10.1016/j.jweia.2017.11.002>.
- [39] Jaramilla B, Huo S. Looking to load and resistance factor rating. *Public Roads* 2005;69.
- [40] Australasian Railway Association. *Bridge Design Code*. Sydney, Australia: Austroads; 1992.